Phosphorylation on Ser5 increases the F-actin-binding activity of L-plastin and promotes its targeting to sites of actin assembly in cells

Bassam Janji[1,*], Adeline Giganti[1,*], Veerle De Corte[2], Marie Catillon[1], Erik Bruyneel[3], Delphine Lentz[1], Julie Plastino[4], Jan Gettemans[2] and Evelyne Friederich[1,‡]

[1]Laboratory for Molecular Biology, Genomics and Modelling, Public Research Centre for Health (CRP-Santé), 84 Val Fleuri, 1526 Luxembourg
[2]Department of Biochemistry, Faculty of Medicine and Health Sciences, Ghent University, Albert Baertsoenkaai 3, 9000 Ghent, Belgium and Flanders Interuniversity, Institute for Biotechnology (V.I.B.), 9052 Ghent, Belgium
[3]Laboratory of Experimental Cancerology, Department of Radiotherapy and Nuclear Medicine, Ghent University Hospital (1P7), De Pintelaan 185, 9000 Ghent, Belgium
[4]Laboratoire Physicochimie "Curie", UMR168 CNRS/Institut Curie, 11, rue Pierre et Marie Curie, 75231 Paris CEDEX 05, France

*These authors contributed equally to this work
‡Author for correspondence (e-mail: Evelyne.Friederich@crp-sante.lu)

Accepted 4 January 2006
Journal of Cell Science 119, 1947-1960 Published by The Company of Biologists 2006
doi:10.1242/jcs.02874

Summary

L-plastin, a malignant transformation-associated protein, is a member of a large family of actin filament cross-linkers. Here, we analysed how phosphorylation of L-plastin on Ser5 of the headpiece domain regulates its intracellular distribution and its interaction with F-actin in transfected cells and in in vitro assays. Phosphorylated wild-type L-plastin localised to the actin cytoskeleton in transfected Vero cells. Ser5Ala substitution reduced the capacity of L-plastin to localise with peripheral actin-rich membrane protrusions. Conversely, a Ser5Glu variant mimicking a constitutively phosphorylated state, accumulated in actin-rich regions and promoted the formation of F-actin microspikes in two cell lines. Similar to phosphorylated wild-type L-plastin, this variant remained associated with cellular F-actin in detergent-treated cells, whereas the Ser5Ala variant was almost completely extracted. When compared with non-phosphorylated protein, phosphorylated L-plastin and the Ser5Glu variant bound F-actin more efficiently in an in vitro assay. Importantly, expression of L-plastin elicited collagen invasion in HEK293T cells, in a manner dependent on Ser5 phosphorylation. Based on our findings, we propose that conversely to other calponin homology (CH)-domain family members, phosphorylation of L-plastin switches the protein from a low-activity to a high-activity state. Phosphorylated L-plastin might act as an integrator of signals controlling the assembly of the actin cytoskeleton and cell motility in a 3D-space.

Supplementary material available online at
http://jcs.biologists.org/cgi/content/full/119/9/1947/DC1

Key words: Fimbrin, Actin bundling, CH-domain, Invasion, Motility

Introduction

Proteins capable of cross-linking actin filaments into networks or bundles play an important role in the assembly of the cellular actin cytoskeleton (Bartles, 2000). In addition, alteration of their functions contributes to pathologies such as cancer, where structural and functional modifications of the actin cytoskeleton accompany uncontrolled cell movement and signalling (Giganti and Friederich, 2003). Regulation of the activities of these proteins by second messengers and post-translational modifications such as phosphorylation allows them to act in a coordinated manner and to build-up specific actin structures in cells.

Initially detected in leucocytes (Matsushima et al., 1988) and cancer cells derived from solid tissues (Goldstein et al., 1985; Lapillonne et al., 2000; Lin et al., 1993a; Lin et al., 1993b; Park et al., 1994) L-plastin was identified as a closely related isoform of intestinal brush-border fimbrin (de Arruda et al., 1990) and is sometimes referred to as L-fimbrin. Several lines of evidence support an important role for L-plastin in the assembly of the actin cytoskeleton. L-plastin is a member of a large family of actin-cross-linking proteins, including α-actinin and filamin (Stossel et al., 2001). Sharing a common actin-binding domain that is made up by two calponin homology (CH)-domains, members of this family control the assembly of most of the actin networks in cells (Gimona et al., 2002). L-plastin and the other plastin isoforms exhibit a modular molecular organisation (de Arruda et al., 1990; Gimona et al., 2002) and similar in vitro activities. The N-terminal calmodulin-like headpiece domain comprises two helix-loop-helix EF-hand Ca^{2+}-binding motifs, followed by two independent actin-binding domains (ABDs) within the same molecule. Cross-linking activity of the other family members requires dimerisation of two polypeptide chains comprising each an ABD. Conversely, the spatially close ABDs (120 Å) of plastins enable them to organise actin-filaments into tight bundles (Bretscher, 1981).

In cells, L-plastin localises to actin-rich membrane structures involved in locomotion, adhesion and immune

defence, including cell-adhesions, immune complexes, filopodia and the phagocytic cup, supporting a role in the organisation of the actin cytoskeleton (Babb et al., 1997; Jones and Brown, 1996; Rosales et al., 1994; Samstag et al., 2003). In line with such a role, overexpression of L-plastin in transfected fibroblast-like CV1 cells induced the rearrangement of focal-adhesion-associated actin filaments (Arpin et al., 1994). L-plastin is also detected in solid tumours of epithelial and mesenchymal origin and was proposed to play a role in tumour cell invasion (Zheng et al., 1999).

Among the three plastin isoforms, L-plastin has the unique property of being phosphorylated in response to signals triggering the activation of the immune response, cell migration and proliferation. L-plastin is phosphorylated on residues Ser5 and Ser7 in hematopoietic cells in vivo, but most likely on Ser5 exclusively in non-hematopoietic cells (Lin et al., 1998; Messier et al., 1993; Shinomiya et al., 1995). Whereas in vivo and in vitro phosphorylation of Ser5 by cAMP-dependent protein kinase A (PKA) is well documented (Lin et al., 1998; Wang and Brown, 1999), there is still controversy over which kinase(s) phosphorylate(s) Ser7.

Importantly, despite the complexity of signalling cascades leading to phosphorylation of L-plastin in immune cells, phosphorylation of this protein occurs upstream of cytoskeleton rearrangements that underly processes such as chemotaxis (Paclet et al., 2004), T cell activation (Henning et al., 1994) or adhesion (Jones and Brown, 1996), suggesting a role for phosphorylated L-plastin in the assembly of actin structures. In support of such a possibility, phosphorylated L-plastin localises to the detergent-insoluble cytoskeletal fraction in adherent macrophages (Messier et al., 1993). However, although it was suggested that phosphorylation of L-plastin regulates its F-actin-binding properties and thus its biological function, experimental support for such a mechanism of regulation is still lacking.

Here, we combined cell biology and biochemical approaches to address the question how phosphorylation regulates the interaction of L-plastin with F-actin. We obtained the first direct evidence that Ser5 phosphorylation of L-plastin promotes its targeting to the actin cytoskeleton and increases its filament bundling activity in cells and in vitro. Importantly, ectopic expression of L-plastin endows epithelial cells with invasive properties in an in vitro collagen invasion assay and this effect depends on Ser5 phosphorylation, suggesting that Ser5 phosphorylated L-plastin contributes to the regulation of cell motility in a 3D-space.

Results

Characterisation of an antibody against L-plastin phosphorylated on Ser5 (Ser5-*P*) and expression of wild-type L-plastin or phosphorylation variants in Vero cells.

Because pharmacological agents such as protein-kinase activators or inhibitors have broad effects on the organisation of the actin cytoskeleton (Howe, 2004), we decided to use a mutational approach to investigate how phosphorylation regulates the biological and biochemical properties of L-plastin (Fig. 1A). We replaced Ser5, its major phosphorylation site that is located in its regulatory headpiece domain (Lin et al., 1998; Shinomiya et al., 1995; Wang and Brown, 1999), with Ala (L-plastin Ser5Ala) or Glu (L-plastin Ser5Glu) to inactivate this site or to mimic constitutive phosphorylation, respectively. Although negatively charged residues and the phosphate group are chemically not identical, it is well documented that this approach can yield valuable information on the biological role of protein phosphorylation (Clarke et al., 2004; Gautreau et al., 2000; Huttelmaier et al., 1999).

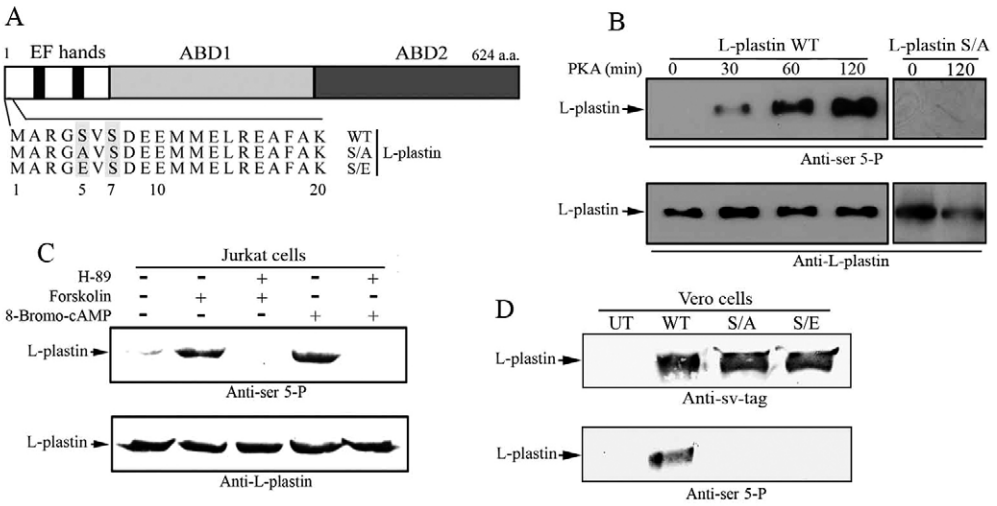

Fig. 1. Characterisation of the L-plastin Ser5 phospho antibody and expression of wild-type L-plastin and phosphorylation variants in Vero cells. (A) Schematic representation of wild-type L-plastin protein (WT) and of phosphorylation variants, and a modular arrangement of L-plastin domains. The amino-acid sequences of the wild-type phosphorylation sites (Ser5 and Ser7) and of the sv-tagged phosphorylation variants (S/A, S/E) are indicated. (B) The anti-Ser5-*P* antibody reacts specifically with in vitro phosphorylated recombinant L-plastin. Equal amounts of recombinant wild-type L-plastin (WT) or or L-plastin Ser5Ala (S/A) were incubated with the catalytic domain of protein kinase A for various time points as described in Materials and Methods. L-plastin was analysed by immunoblotting with anti-Ser5-*P* (upper panel) or anti-L-plastin antibodies (lower panel). (C) The anti-Ser5-*P* antibody specifically reacts with phosphorylated L-plastin in Jurkat T lymphoid cells. Jurkat cells were stimulated with 1 mM 8-Bromo-cAMP or 0.1 mM forskolin for 45 minutes. Before stimulation, cells were treated (+) or not (–) with 50 μM of H-89 for 45 minutes. Equal amounts of cell lysates were analysed by immunoblotting with anti-Ser5-*P* (upper panel) or anti-L-plastin antibodies (lower panel). (D) Expression and Ser5 phosphorylation of wild-type L-plastin and phosphorylation variants in Vero cells. Vero cells were transfected with cDNA constructs encoding sv-tagged wild-type (WT), Ser5Ala (S/A) or Ser5Glu (S/E) L-plastin. Untransfected cells (UT) were used as a negative control. After 48 hours, equal amounts of cell extracts were analysed by immunoblotting. Transfected proteins were detected with anti-sv-tag (upper panel) or anti-Ser5-*P* antibodies (lower panel).

To analyse phosphorylated wild-type L-plastin in cells, we raised an antibody against a synthetic phospho-peptide encompassing the phosphorylation site of L-plastin and harbouring a phosphate group on Ser5 (anti-Ser5-*P* antibody). To test the specificity of this antibody, we first took advantage of the observation that protein kinase A (PKA) exclusively phosphorylates wild-type L-plastin on Ser5 in vitro (Jones et al., 1998; Wang and Brown, 1999). Immunoblotting with anti-Ser5-*P* of in-vitro-phosphorylated recombinant L-plastin, revealed a time-dependent increase in signals (Fig. 1B, upper panel) whereas signals remained constant when the same samples were analysed with anti-L-plastin antibody (B, lower panel). Anti-Ser5-*P* did not react with Ser5Ala L-plastin incubated in the presence of PKA (B, upper panel, L-plastin S/A).

We used Jurkat T lymphoid cells to determine whether this antibody also allowed us to distinguish between the phosphorylated and non-phosphorylated forms of L-plastin in cell extracts. Whereas in non-stimulated Jurkat cells base-line phosphorylation of L-plastin is barely detectable, activation of PKA greatly increases phosphorylation on Ser5 (Jones et al., 1998; Wang and Brown, 1999). Jurkat cells expressed high amounts of endogenous L-plastin – as revealed with the anti-L-plastin antibody (Fig. 1C, lower panel). A faint signal was detected with anti-Ser5-*P* antibody in non-stimulated cells that greatly increased when cells were stimulated with the PKA activators forskolin or 8-Bromo-cAMP (Fig. 1C, upper panel). Conversely, no protein band was detected when cells were pre-incubated with a PKA inhibitor H-89 prior to stimulation (Fig. 1C, upper panel). In all cases, the total amount of L-plastin did not vary (Fig. 1C, lower panel). This result clearly showed that the anti-Ser5-*P* antibody specifically reacted in vivo with L-plastin phosphorylated at Ser5 but not with the non-phosphorylated form.

We first used fibroblast-like Vero cells, which exhibit a well-organised actin cytoskeleton, as a model system to study the role of L-plastin phosphorylation on Ser5 in transfection experiments. Notably, Vero cells do not produce L-plastin, as determined with an anti-L-plastin antibody (data not shown). Vero cells were transfected with wild-type L-plastin or L-plastin Ser5-substitution variants epitope-tagged with the 13 C-terminal residues of the Sendai virus L protein (sv-tag). Expression and phosphorylation of wild-type and mutants was then monitored by immunoblotting of the different cell lysates (Fig. 1D). Similar amounts of wild-type L-plastin or of its Ser5-substitution variants were produced in Vero cells (Fig. 1D, upper panel). However, probing the same cell lysates with anti-Ser5-*P* antibody, revealed a band in wild-type-transfected cells but not in those transfected with the Ser5-substitution variants (Fig. 1D, lower panel). This result further highlighted the specificity of the anti-Ser5-*P* antibody and showed that L-plastin was phosphorylated on Ser5 in Vero cells, as previously reported for related cell types (Lin et al., 1998).

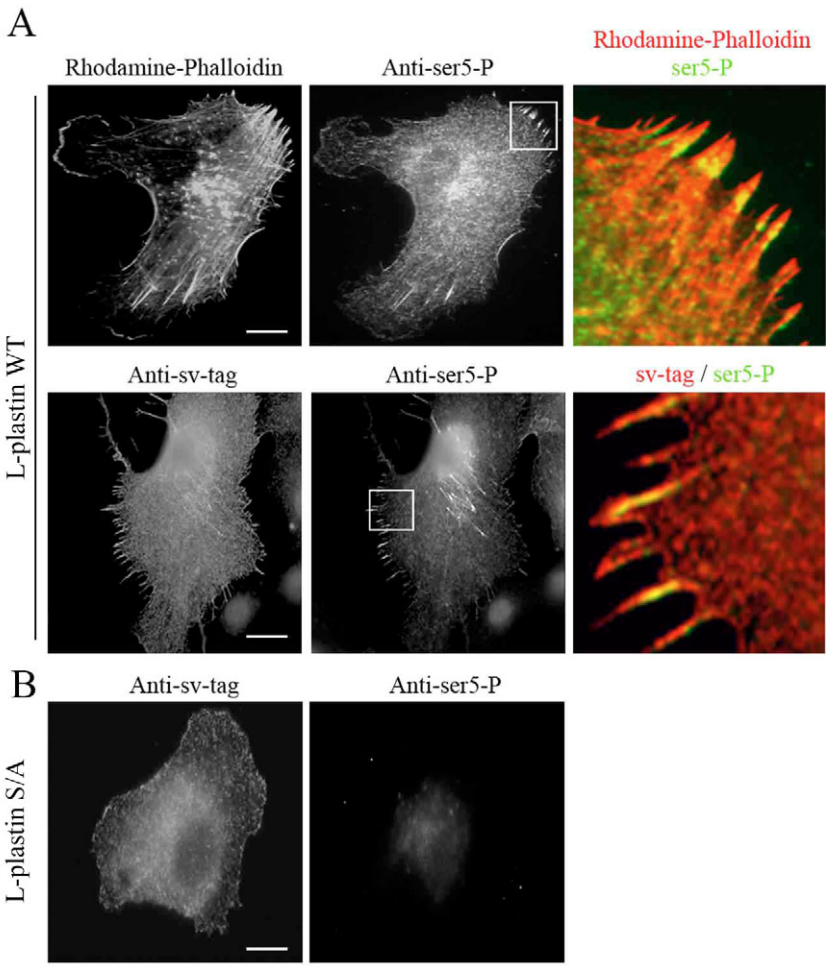

Fig. 2. L-plastin phosphorylated on Ser5 localises to the actin cytoskeleton in Vero cells. Transfected Vero cells expressing wild-type L-plastin or S/A variant were processed for immunofluorescence staining. (A) Intracellular distribution of L-plastin phosphorylated on Ser5. (Upper row) Cells expressing wild-type L-plastin (WT) were stained with Rhodamine-phalloidin (left panel) and anti-Ser5-*P* antibody (middle panel). Alexa-Fluor-488-coupled anti-rabbit IgG antibody served as secondary antibody. Merged image of enlarged regions (boxes) of left and middle images is shown on the right. Red, F-actin; green, anti-Ser5-*P* antibody. (Lower row) Cells expressing wild-type L-plastin were double-stained with anti-sv-tag antibody (left panel) and anti-Ser5-*P* antibody (middle panel) with Alexa-Fluor-594-coupled anti-mouse and Alexa-Fluor-488-coupled anti-rabbit IgG antibody as secondary antibodies, respectively. Merged image of enlarged regions (boxes) of left and middle images is shown on the right. Red, total WT L-plastin; green, phosphorylated WT L-plastin. Bars, 15 μm. (B) The anti-Ser5-*P* antibody does not react with Ser5Ala L-plastin. Cells expressing the non-phosphorylatable Ser5Ala variant (S/A) were double-stained with anti-sv-tag antibody (left) and anti-Ser5-*P* antibody (right) as described above. Bar, 15 μm.

L-plastin phosphorylated on Ser5 localises to the actin cytoskeleton in Vero cells

We first investigated the intracellular distribution of L-plastin phosphorylated on Ser5 (Ser5-*P*-plastin) in transfected Vero cells (Fig. 2). Immunofluorescence analysis with anti-Ser5-*P*

antibody and Rhodamine-phalloidin as a probe for F-actin revealed that most of Ser5-*P*-plastin localised to F-actin-rich structures, including membrane ruffles and microspikes found at the cell periphery (Fig. 2A, upper panels). In addition, Ser5-*P*-plastin also weakly decorated stress fibres, frequently located in the centre of the cell. Co-staining of cells expressing L-plastin by using anti-Ser5-*P* antibody and an antibody against the sv-tag as probes for the total pool of L-plastin, revealed similar but not identical staining patterns (Fig. 2A, lower panels). In addition to the cytoskeleton-associated pool of L-plastin that was also detected by the anti-Ser5-*P* antibody, the anti-sv-tag antibody revealed a more intense cytoplasmic staining, suggesting that most of cytosplasmic L-plastin was not phosphorylated (Fig. 2A, left panel). The anti-Ser5-*P* antibody did not react with non-phosphorylable L-plastin containing the Ser5Ala mutation, confirming the specificity of the staining (Fig. 2B).

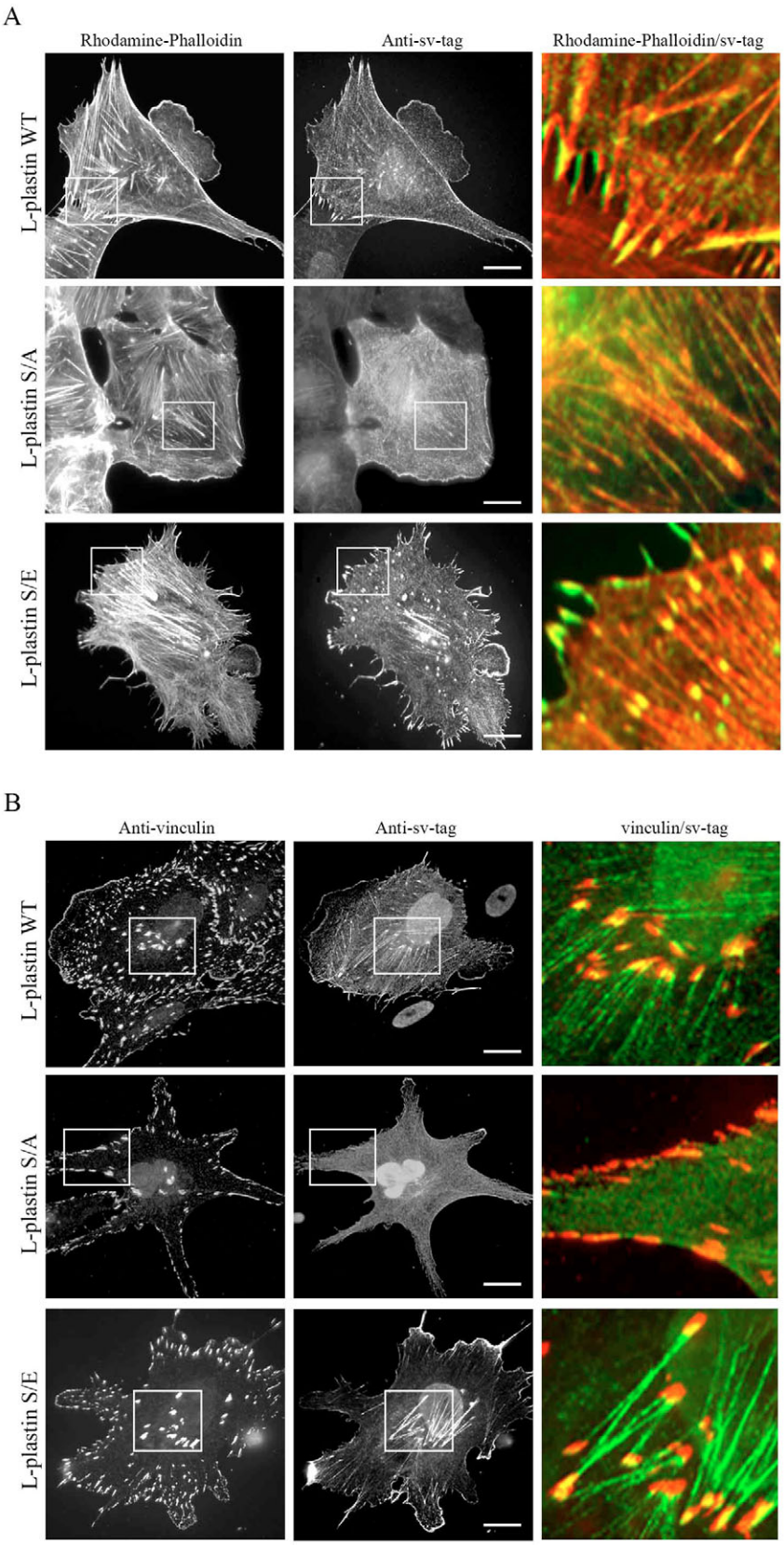

Intracellular localisation of L-plastin Ser5-phosphorylation variants.

To examine whether Ser5 phosphorylation regulates the interaction of L-plastin with the cellular actin cytoskeleton, we compared the intracellular distribution of L-plastin phosphorylation variants in transfected Vero cells (Fig. 3). Wild-type L-plastin co-distributed with F-actin in peripheral microspikes and membrane protrusions and also decorated the proximal, membrane-anchored end of stress fibres (Fig. 3A, upper panels). By marked contrast, L-plastin Ser5Ala (Fig. 3A, middle panels) exhibited little co-distribution with these F-actin structures and a diffuse cytoplasmic staining. Notably, L-plastin Ser5Ala-Ser7Ala, a variant in which both potential phosphorylation sites were invalidated, yielded a similar phenotype (data not shown). Conversely, L-plastin Ser5Glu (Fig. 3A, lower panels) predominantly localised to peripheral

Fig. 3. Intracellular distribution of L-plastin phosphorylation variants in Vero cells. (A,B) Transfected Vero cells expressing wild-type L-plastin (upper rows), L-plastin Ser5Ala (middle rows) or L-plastin Ser5Glu (lower rows) were processed for immunofluorescence double-staining. (A) Co-distribution of L-plastin variants with F-actin. Cells were stained with Rhodamine-phalloidin (left column) and anti-sv-tag antibody (middle column). Secondary antibody as in Fig. 2A. Merged images of enlarged regions (boxes) of left and middle images are shown on the right. Red, F-actin; green, total L-plastin. Bars, 15 μm. (B) Co-distribution of L-plastin variants with vinculin. Cells were double-stained with vinculin (left column) and sv-tag antibody (middle column). Secondary antibodies as in Fig. 2A. Merged images of enlarged regions (boxes) of left and middle images are shown on the right. Red, vinculin; green, total L-plastin. Bars, 15 μm.

membrane protrusions and the number of spike-like actin structures detectable in these cells was increased sixfold when compared with cells producing the Ser-Ala variant. In addition, similar to wild-type L-plastin, the Ser5Glu variant decorated a subset of stress fibers, mostly located in the centre of the cell.

The dot-like staining pattern observed with L-plastin Ser5Glu was reminiscent of that of cell-matrix adhesions. Co-staining of cells with vinculin as a marker for focal adhesions, showed that wild-type L-plastin and the Ser5Glu variant strongly colocalised with the distal, actin-associated portion of these structures. Of note, this staining pattern was most prominent in the cell centre (Fig. 3B, upper and lower rows). By contrast, Ser5Ala only weakly co-distributed with vinculin (B, middle row).

The prominent label in peripheral membrane extensions suggested that phosphorylated L-plastin and the Ser5Glu variant might target to sites of actin assembly (Pollard and Borisy, 2003). To confirm this, Vero cells expressing wild-type L-plastin or its phosphorylation variants were co-stained for the Arp2/3-complex-binding protein cortactin (Weed et al., 2000), used here as a marker for sites of actin polymerisation (Fig. 4). Cortactin concentrates in peripheral membrane extensions of migrating cells, such as lamellipodia (Bryce et al., 2005) and podosomes (Mizutani et al., 2002), and ventral membrane protrusions found in various cell types, including invasive cancer cells (Linder and Aepfelbacher, 2003). Cortactin co-distributed with Ser5Glu L-plastin (Fig. 4, upper panels) in peripheral plasma membrane extensions but not in dot-like structures. Triple staining of cells expressing wild-type L-plastin revealed that also Ser5-*P*-plastin co-distributed with cortactin in actin-rich plasma membrane extensions (Fig. 4, middle panels), but to a lesser extend when compared with the Ser5Glu variant. Conversely, Ser5Ala L-plastin (Fig. 4, lower panels) showed no significant co-distribution with cortactin. These results suggested that part of the phosphorylated pool of L-plastin localised to sites of Arp2/3-complex-mediated actin assembly. Although phosphorylated L-plastin was previously shown to co-distribute with vimentin in macrophages (Correia et al., 1999), we were unable to detect a co-distribution of both proteins in Vero cells (supplementary material Fig. S1).

To confirm that Ser5Glu stabilised peripheral actin-structures, we next analysed the effects of phosphorylation variants in LLCPK1 epithelial kidney cells that were previously used to assess the role of F-actin bundling proteins in the assembly of the cortical actin cytoskeleton (Arpin et al., 1994; Friederich et al., 1989; Loomis et al., 2003). In addition to stress fibres and micro-spikes present at their basal surface, these cells harbour numerous spike-like actin structures at their apical face, corresponding to the core bundles of microvilli. Elongation of these structures caused by forced expression of

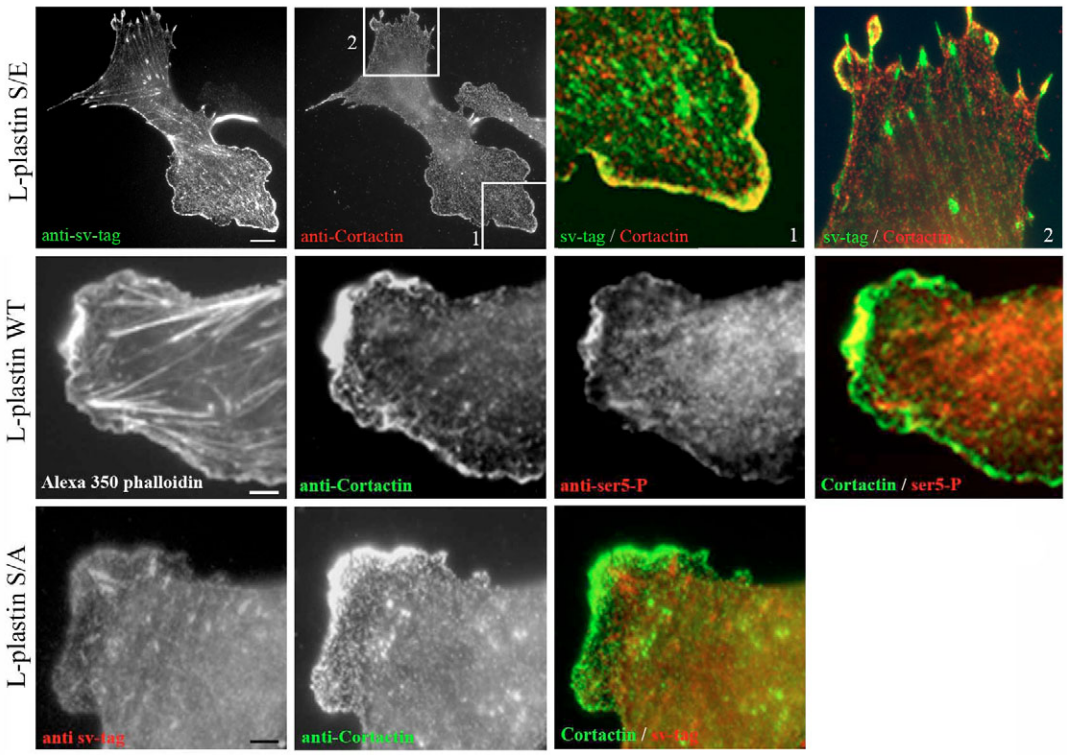

Fig. 4. Targeting of phosphorylated L-plastin to areas of fast actin assembly. Transfected Vero cells expressing Ser5Glu (S/E), Ser5Ala (S/A) or wild-type L-plastin were processed for immunofluorescence double- or triple-staining. (Upper row) Cells expressing Ser5Glu variant were double-labelled with anti-cortactin and anti-sv-tag antibodies. Alexa-Fluor-488-coupled anti-mouse IgG (L-plastin S/E, green) and Texas-Red-coupled anti-rabbit IgG antibody (cortactin, red) served as secondary antibodies. The two right panels show merges of enlarged regions (boxes) of anti-sv-tag- and anti-cortactin-stained images. Bar, 15 μm. (Middle row) Cells expressing wild-type L-plastin were triple-labelled with Alexa-Fluor-350-phalloidin, anti-cortactin and anti-Ser5-*P* antibodies. Alexa-Fluor-488-coupled anti-mouse IgG (cortactin, green) and Texas-Red-coupled anti-rabbit IgG antibody (Ser5-*P* WT L-plastin, red) served as secondary antibodies. The right panel shows a merge of cortactin and anti-Ser5-*P* staining. Bar, 3 μm. (Lower row) Cells expressing L-plastin Ser5Ala were labelled with anti-cortactin and anti-sv-tag antibody. Secondary antibodies were used as described above (middle row). The right panel shows a merge of cortactin and sv-tag images. Bar, 3 μm.

bundling proteins can be easily visualised by epifluorescence microscopy. A focal plane on the apical surface of these cells revealed that Ser5Glu mutants strongly colocalised with the F-actin bundles of surface microvilli that were more prominent than those detected in non-transfected neighbouring cells (Fig. 5, upper and lower panels). By marked contrast, the Ser5Ala variant exhibited a diffuse cytoplasmic distribution and its association with these surface projections was barely detectable (Fig. 5, middle panels). This result suggest that Ser5Glu L-plastin stabilises and/or bundles actin filaments of plasma membrane protrusions.

L-plastin phosphorylation on Ser5 increases its avidity for cellular F-actin.

Immunolocalisation studies with wild-type L-plastin and its phosphorylation variants suggested that the phosphorylated form bound more tightly to the actin cytoskeleton. To test this, we treated cells with Triton X-100, a non-ionic detergent, prior to fixation and processing for immunofluorescence staining. This approach allows to evaluate of the avidity of actin-binding proteins for different F-actin structures in the context of the cell (Arpin et al., 1994; Friederich et al., 1992). Whereas membrane and cytosolic proteins are extracted, proteins that are tightly associated with the actin cytoskeleton remain bound. Wild-type L-plastin remained associated with F-actin structures in detergent-extracted transfected Vero cells (Fig. 6A, upper panels), as previously reported (Arpin et al., 1994; Friederich et al., 1992). Like wild-type L-plastin, the Ser5Glu variant remained associated with actin cytoskeleton (Fig. 6A, lower panels). Conversely, L-plastin Ser5Ala was almost totally extracted. In a few cells, we detected residual labelling, restricted to the ends of stress fibres and peripheral microspikes (Fig. 6A, middle panels). In line with this qualitative result, the number of cells exhibiting detectable cytoskeleton-associated Ser5Ala staining decreased on average by 83% after detergent-extraction, wheras detectable signals decreased only by 50% for cells transfected with wild-type or Ser5Glu L-plastin (Fig. 6B). These results suggest that the Ser5Ala variant has a reduced avidity for cellular F-actin. The detergent-resistant pool of wild-type L-plastin was phosphorylated on Ser5 (Fig. 6C).

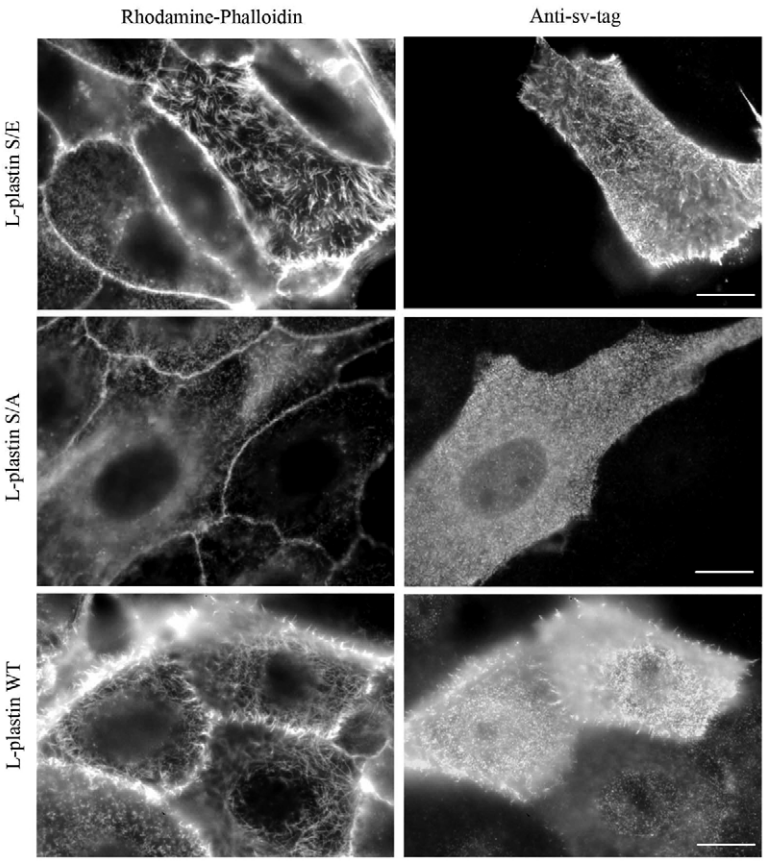

Fig. 5. Targeting of L-plastin phosphorylation variants to surface-F-actin spikes in epithelial LLCPK1 cells. LLCPK1 cells expressing Ser5Glu (S/E, upper panels), Ser5Ala (S/A, middle panels) or WT L-plastin (WT, lower panels) were double-stained with Rhodamine-phalloidin (left panels) and anti-sv-tag antibody (right panels). Cy2-coupled anti-rabbit IgG served as secondary antibody. Bars, 15 μm.

Ser5 phosphorylation increases the F-actin-binding activity of L-plastin in vitro.

Taken together, these results indicate that Ser5 phosphorylation of L-plastin positively regulates its association with F-actin. Therefore, we next compared F-actin-binding properties of non-phosphorylated and PKA-phosphorylated L-plastin in a co-sedimentation assay with F-actin in vitro (Fig. 7A). At a L-plastin to actin ratio of 1:2, almost twice as much phosphorylated L-plastin co-sedimented with F-actin compared with the non-phosphorylated form (Fig. 7B). Immunoblotting analysis with anti-Ser5-*P* confirmed that L-plastin in pellets was phosphorylated on Ser5 (Fig. 7C). As expected, Ser5-*P* signals increased as a function of L-plastin concentration, correlated with the increase of L-plastin in the pellets (Fig. 7C). Similar to non-phosphorylated wild-type L-plastin, also the Ser5Ala variant bound F-actin in vitro (Fig. 7B and supplementary material Fig. S2), suggesting that the Ser5 Ala substitution did not grossly affects F-actin binding.

In vitro phosphorylation of wild-type protein is prone to experimental variations and the extend to which the protein is phosphorylated is difficult to quantify. Therefore, we decided to use the Ser5Glu variant in further in vitro studies. In agreement with previous results (Namba et al., 1992), non-phosphorylated wild-type L-plastin bound F-actin in a dose-dependent manner (Fig. 7A), and the data fitted a hyperbolic function (Fig. 7B). Interestingly, the Ser5Glu variant exhibited a different binding curve and distinct saturation behaviour compared with non-phosphorylated wild type (Fig. 7B). Whereas similar amounts of wild-type L-plastin and the Ser5Glu variant bound at low molar ratios of plastin to actin, almost twice as much Ser5Glu variant bound at a high plastin to actin ratio (1:2), and F-actin binding saturation was not reached for this variant.

Bundling activity of L-plastin was assessed in a low-speed centrifugation assay allowing to sediment F-actin bundles but not single filaments (Glenney, Jr et al., 1981). Importantly, Ser5Glu L-plastin had

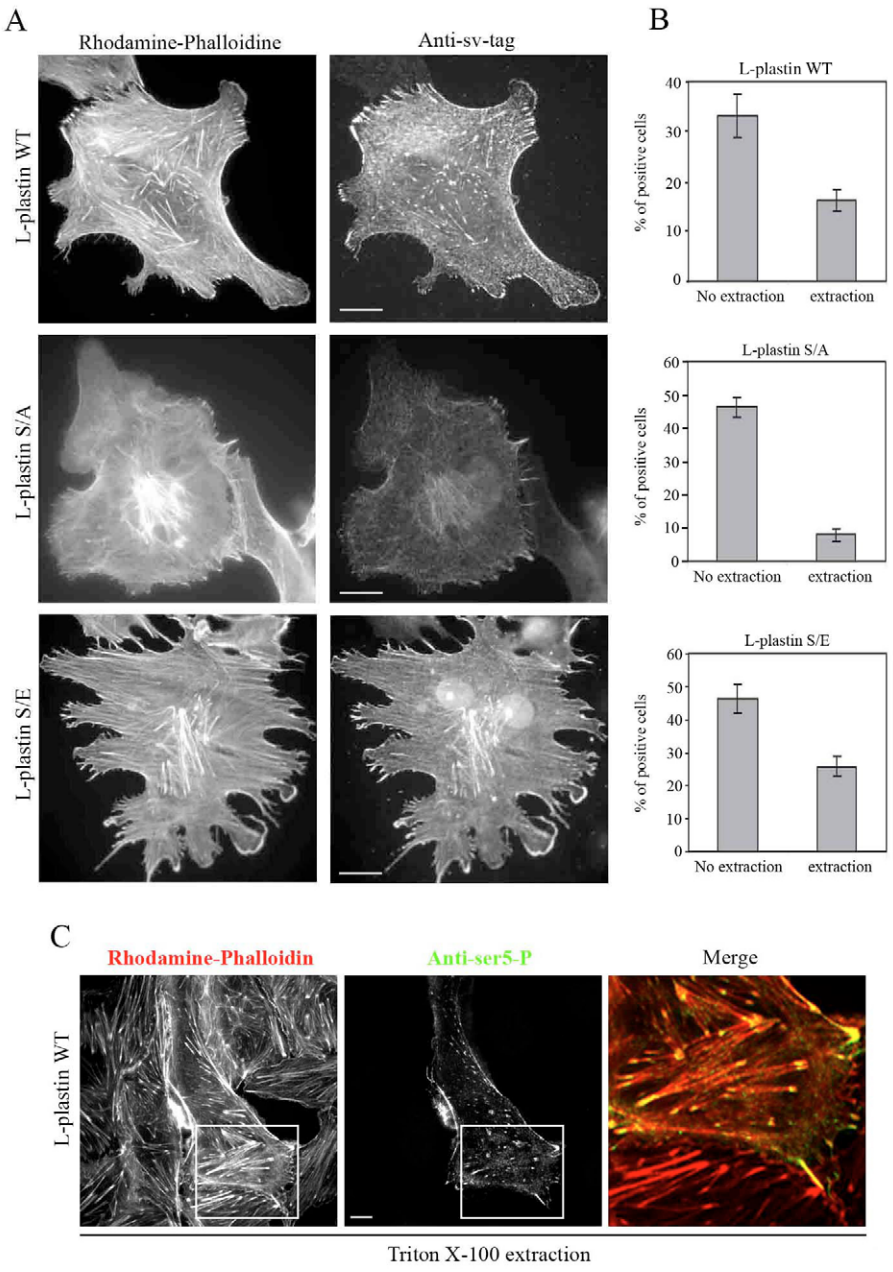

Fig. 6. Probing the avidity of L-plastin phosphorylation variants for cellular actin structures by detergent extraction. (A) Immunolocalisation of L-plastin variants after detergent extraction. Transfected Vero cells expressing L-plastin wild-type (upper panels), Ser5Ala (middle panels) or Ser5Glu (lower panels) were extracted with Triton X-100 prior to fixation. Cells were stained with anti-sv-tag antibody (right row) and Rhodamine-phalloidin (left row) as described in Fig. 3A. Bars, 15 μm. (B) Quantification of extraction experiments. Cells exhibiting a sv-positive staining pattern were counted on untreated (no extraction) and detergent-extracted (extraction) coverslips, as described in Materials and Methods. (C) Immunolocalisation of phosphorylated wild-type L-plastin after detergent extraction. Transfected Vero cells expressing wild-type L-plastin were extracted as described in A and stained with Rhodamine-phalloidin (left panel) and anti-Ser5-*P* antibody (middle panel). Right panel shows a merge of enlarged regions (boxes) of left and middle images. Green, Ser5-*P* WT L-plastin; red, F-actin. Bar, 15 μm.

markedly higher bundling activity (Fig. 8), even at low plastin to actin ratios, where no differences in F-actin binding was observed (Fig. 8B). At a molar ratio of 1:8, 47% of F-actin sedimented when non-phosphorylated L-plastin was added, whereas 84% of F-actin pelleted in the presence of the Ser5Glu variant (Fig. 8B). Formation of F-actin bundles was confirmed by transmission electron microscopy (Fig. 8C). Whereas only a few F-actin bundles were detected in the presence of non-phosphorylated L-plastin (Fig. 8C, left panel), F-actin preparations incubated with Ser5Glu variant exhibited a large number of tight F-actin bundles (Fig. 8C, right panel). Because Ser5 is spatially close to the EF-hand Ca^{2+}-binding motif of the headpiece domain, we wanted to determine whether the presence of a negatively charged group at amino acid position 5 interfered with the inhibitory effect of Ca^{2+} (Namba et al., 1992). In pellets, an almost identical decrease in F-actin was observed at low-speed centrifugation when non-phosphorylated wild-type L-plastin or the Ser5Glu variant were incubated in the presence of increasing concentrations of free Ca^{2+} (Fig. 8D), suggesting that addition of a negative charge in amino acid position 5 does not influence Ca^{2+}-dependency of F-actin bundling.

Since Ser5-*P*-plastin is targeted to peripheral membrane protrusions and focal adhesions known to be involved in cell migration, we tested whether L-plastin affects cell migration in a phosphorylation-dependent manner. Since L-plastin has been associated with cell invasion (Zheng et al., 1999), we expressed wild-type L-plastin or phosphorylation variants in human embryonic kidney HEK293T cells that do not produce endogenous L-plastin (data not shown) and investigated their invasive capacity in an in vitro collagen assay (Bracke et al., 2001; De Corte et al., 2002). This semi-quantitative assay

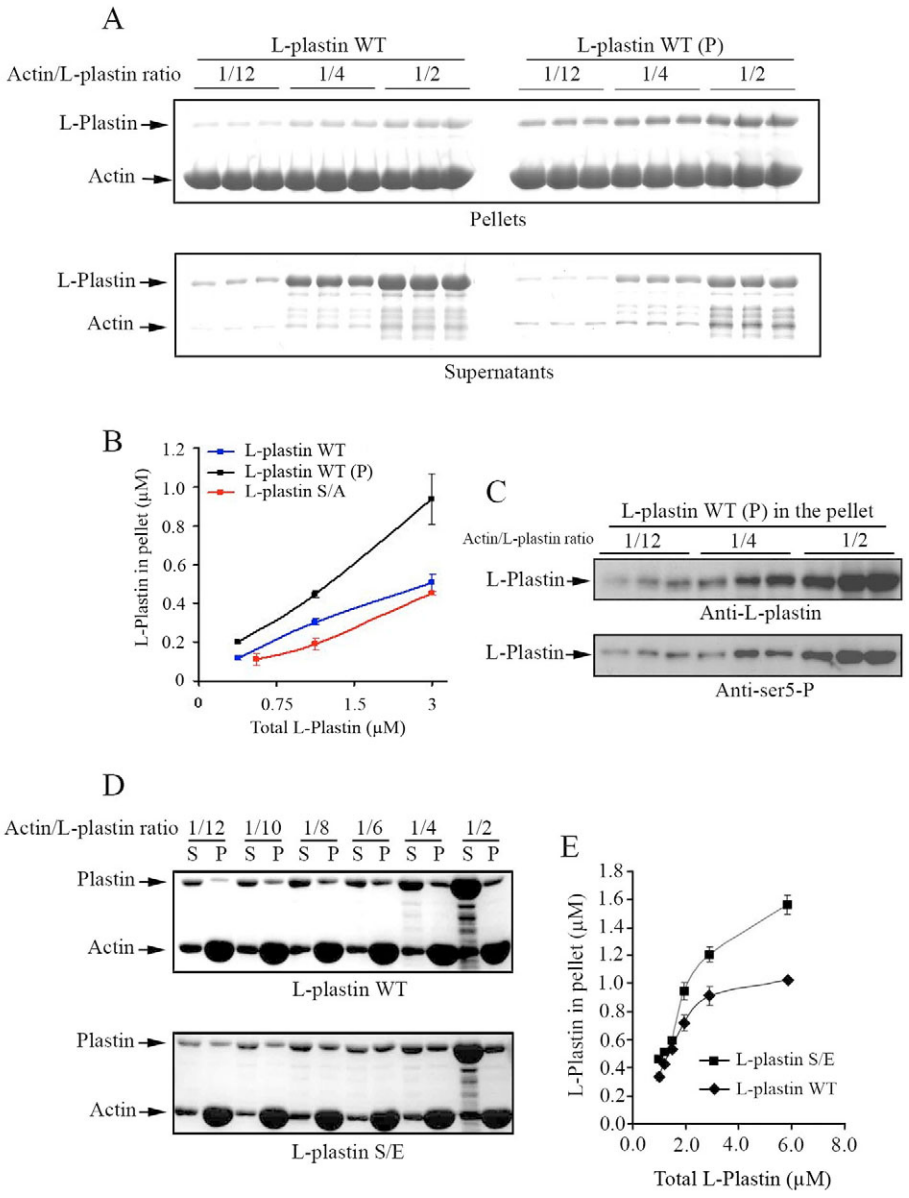

Fig. 7. Phosphorylated wild-type L-plastin and S/E variant bind with a higher stoichiometry to F-actin than non-phosphorylated wild-type protein. (A) Binding of phosphorylated and non-phosphorylated wild-type L-plastin to F-actin. Wild-type L-plastin (L-plastin WT) was incubated in the absence or presence of the catalytic domain of PKA for 120 minutes at 30°C. G-actin (6 μM) was copolymerised with various concentrations of phosphorylated [L-plastin WT (P)] or non-phosphorylated wild-type L-plastin (L-plastin WT) and centrifuged at high speed. Supernatants and pellets were analysed by SDS-PAGE. Coomassie-staining patterns of pellets (top panel) and supernatants (bottom panel) of triplicate samples are shown. The molar ratios of L-plastin to actin are indicated. (B) Quantification of binding of phosphorylated or non-phosphorylated wild-type L-plastin and L-plastin S/A variant to F-actin. Amounts of phosphorylated (black) or non-phosphorylated (blue) wild-type L-plastin and L-plastin S/A variant (red) in pellets and supernatants were quantified by densitometry of Coomassie-stained protein bands. L-plastin in the pellets is plotted as a function of increasing L-plastin concentrations. Each point is the mean of three experiments ± s.d. (C) Immunoblotting analysis of phosphorylated wild-type L-plastin, co-sedimented with F-actin. A fraction of protein pellets shown in A (upper panel) was analysed by immunoblotting using anti-Ser5-*P* antibody (lower panel). After stripping the membrane, total L-plastin was detected with anti-L-plastin antibody (upper panel). Triplicate samples are shown for each actin to plastin ratio. (D) Binding of WT L-plastin and S/E variant to F-actin. G-actin (12 μM) was copolymerised with various concentrations of WT L-plastin or S/E variant and centrifuged at high speed. Coomassie-staining patterns of supernatants (S) and pellets (P) are shown. The molar ratios of L-plastin to actin are indicated. (E) Binding curves of WT L-plastin or S/E variant to F-actin. Amounts of F-actin-bound WT L-plastin (rhombus) and S/E variant (square) in the pellet are plotted as a function of increasing L-plastin concentrations. Each point is the mean of four experiments ± s.d.

measures to what extent cells can migrate through a 3D-collagen gel and mimic invasion of tumour cells in the stroma. Immunoblotting analysis of transfected HEK293T cells revealed that similar amounts of L-plastin variants were produced (Fig. 9A). Untransfected wild-type HEK293T cells are not invasive, in contrast to DHD-FIB rat colon myofibroblasts that were used as a positive control (Fig. 9B). We observed that expression of the wild-type L-plastin conferred invasive properties to HEK293T cells in this assay. Importantly, cells producing the Ser5Ala variant behaved like non-transfected control cells. Conversely, similar to wild-type L-plastin, the Ser5Glu variant endowed cells with invasive properties (Fig. 9B). These findings suggested that L-plastin phosphorylation at Ser5 is a prerequisite to elicit collagen invasion. Invasion of epithelial cells is associated in part with loss of cell-cell adhesion contacts. To investigate the effects of wild-type L-plastin and variants on cell-cell contact formation, we used a fast cell aggregation assay in which cells are cultured in suspension and their capacity to form aggregates is evaluated (Boterberg et al., 2001; De Corte et al., 2002). Non-invasive cells are expected to form larger aggregates than invasive cells. HEK293T cells transfected with wild-type L-plastin or the Ser5Glu variant showed drastic reduction in particle size (~10 to 100 μm) at 30 minutes of culture (Fig. 9C) to a size comparable to mock-transfected cells at time zero (see arrow Fig. 9C). The particle diameter of HEK293T cells transfected with Ser5Ala or Ser5Ala-Ser7Ala at 30 minutes of culture was much larger (~100 to 1500 μm) and comparable to that of mock-transfected (MT) cells at 30 minutes. Conversely to the collagen invasion assay, cells transfected with L-plastin

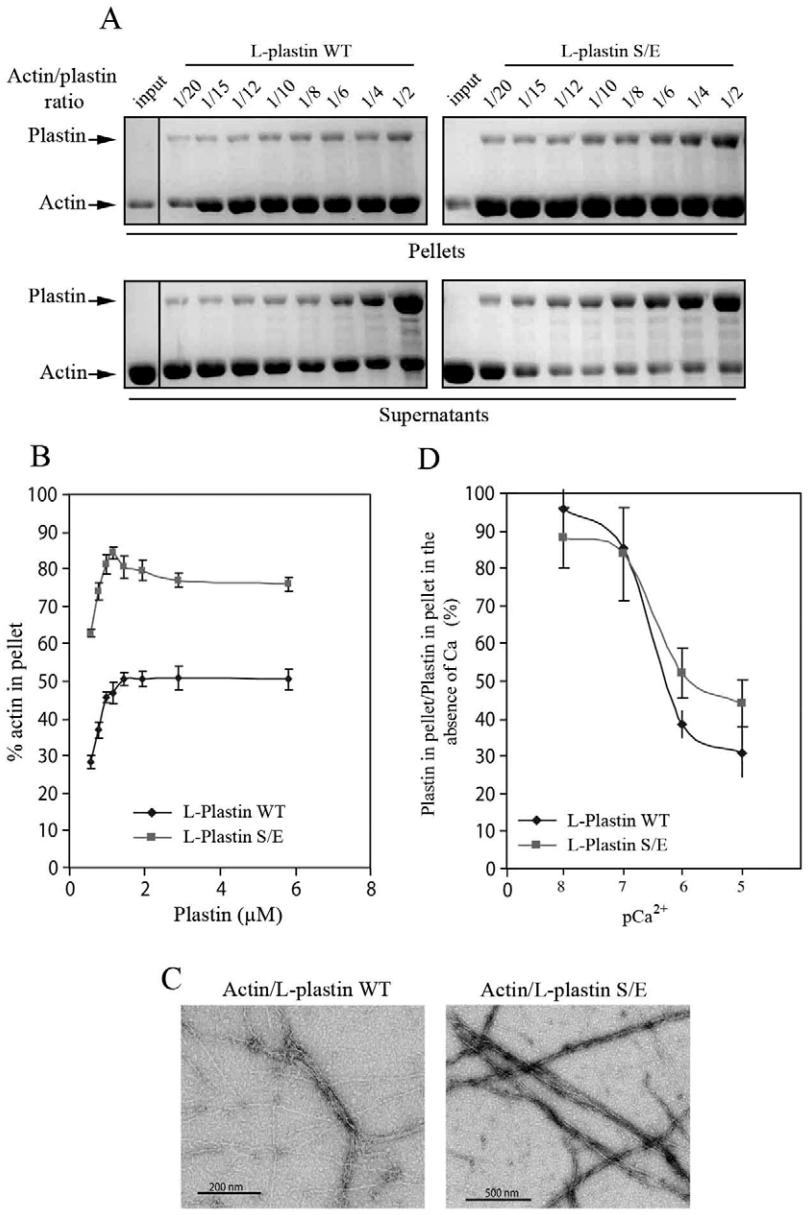

Fig. 8. L-plastin Ser5Glu has highly increased bundling activity when compared to non-phosphorylated wild type protein. (A) Co-sedimentation of WT L-plastin or S/E variant with F-actin bundles. Co-sedimentation of 12 μM G-actin with WT L-plastin or S/E variant as described in Fig. 7, with the exception that mixtures were centrifuged at low speed to sediment F-actin bundles. Coomassie-staining patterns of pellets (upper panels) and supernatants (lower panels) are shown. Lane 1, actin alone (input). The molar ratios of L-plastin to actin are indicated. (B) Quantification of F-actin bundle formation. Actin in the pellet (% of total) corresponding to bundled F-actin, was plotted as a function of increasing concentrations of WTL-plastin (◆) or L-plastin Ser5Glu (■). Each point is the mean of four experiments ± s.d. (C) Electron microscopy reveals increased bundle formation in the presence of S/E variant. Actin was co-polymerised with L-plastin WT (left) or L-plastin S/E (right) at a molar ratio of 1:4 as described in A. Actin filaments were negatively stained with 1% uranyl acetate and analysed by transmission electron microscopy. Electron microscopy images are shown. (D) Effect of Ca^{2+} on bundling activities of L-plastin WT or S/E variant. Low-speed co-sedimentation of 12 μM G-actin with L-plastin WT (◆) or S/E variant (■) was performed as described in A, at a 1:4 molar ratio, in the presence of various concentrations of Ca^{2+}. pCa was varied by the addition of various volumes of 1 mM $CaCl_2$. pCa=8 (0.024 mM); pCa=7 (0.195 mM); pCa=6 (0.709 mM); pCa=5 (0.971 mM). Note that pCa=–log [Ca^{2+}]. F-actin in the pellet (% of total) was plotted as a function of increasing concentrations of free Ca^{2+}. Each point is the mean of three experiments ± s.d.

variants behaved similar when tested in a migration assay on plastic dishes. HEK293T cells were grown to confluency and after 48 hours, a wound was made by scratching a line in the cell monolayer. When analysing the capacity of cells to migrate into the wounds, no significant difference could be measured for cells transfected with the various constructs (Fig. 9D).

Because L-plastin is a well-characterised, direct downstream target of PKA in hematopoietic cells (Wang and Brown, 1999), we determined whether PKA inhibitors affected L-plastin-dependent collagen invasion. Whereas PKA inhibition strongly reduced L-plastin-dependent cell invasion, PKC inhibitors did not affect this process (Fig. 9E). To confirm that PKA indeed phosphorylated wild-type L-plastin in HEK293T cells, L-plastin-transfected cells were treated with the cell-permeable PKA activator 8-Bromo-cAMP (Fig. 9F). When compared with untreated cells, 8-Bromo-cAMP stimulated L-plastin phosphorylation, as monitored by the threefold increase of the signal detected with anti-Ser5-*P* antibody (Fig. 9F). Incubation of cells in the presence of PKA inhibitor prior to 8-Bromo-cAMP addition inhibited this stimulation (Fig. 9F), without, however, inhibiting base-line phosphorylation of L-plastin.

Taken together, these results show that phosphorylated L-plastin affects cell migration in a 3D- but not in a 2D-space and that PKA-elicited signalling is required for L-plastin-mediated invasion.

Discussion

L-plastin, a major F-actin-bundling protein of leucocytes and epithelial- or mesenchymal-derived cancer cells, is phosphorylated upon activation of pathways triggering adhesion and migration, concomitantly to remodelling the actin (Henning et al., 1994; Matsushima et al., 1988; Shibata et al., 1993; Wang and Brown, 1999). Here, we gained consistent evidence that phosphorylation of L-plastin positively regulates its F-actin-binding and cross-linking activities and that it might function as a regulatory switch in the assembly of actin-rich

structures involved in cell migration and signalling. Importantly, phosphorylated L-plastin might contribute to the regulation of the migratory behaviour of cells in a 3D-space.

In line with previous data (Lin et al., 1998), we found that L-plastin is phosphorylated on Ser5 in fibroblast-like Vero cells and epithelial HEK293T cells. Conversely to Jurkat T lymphoid cells, Vero and HEK293T cells exhibited high-baseline phosphorylation of L-plastin on Ser5. Whereas

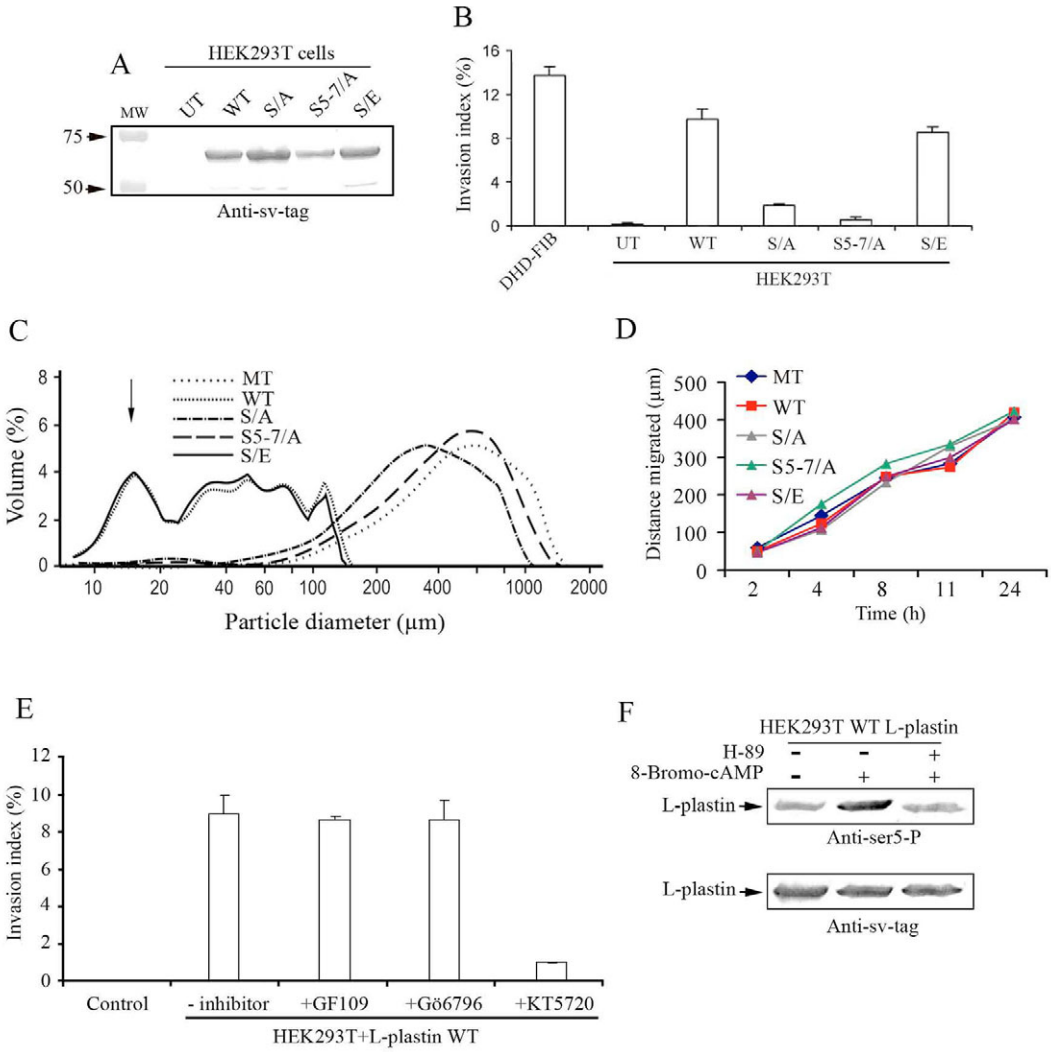

Fig. 9. Ser-Ala substitution in L-plastin is sufficient to abolish L-plastin-dependent collagen invasion. (A) Expression of wild-type L-plastin and phosphorylation variants in HEK293T cells. HEK293T cells were transfected with cDNA constructs encoding wild type (WT), Ser-Ala (S/A), Ser5Ala-Ser7Ala (S5-7/A) or Ser5Glu L-plastin (S/E). Untransfected cells were used as a negative control (UT). After 48 hours, equal amounts of cell extracts (20 μg) were analysed by immunoblotting with anti-sv-tag antibody. (B) Collagen-invasion-capacity of HEK293T cells expressing WT L-plastin or phosphorylation variants. Transfected cells expressing wild-type L-plastin or L-plastin phosphorylation variants were tested for their capacity to invade a collagen-type-I gel as described in Materials and Methods. DHD-FIB rat colon myofibroblasts were used as positive control for invasion and untransfected (UT) HEK293T cells as negative control. Results are representative of three independent experiments (mean ± s.d.). (C) Fast aggregation assay of HEK293T cells transfected with WT L-plastin and phosphorylation variants. Plotted curves of relative volume distribution (*y*-axis) as a function of particle diameter (*x*-axis) are shown for mock-transfected (MT) HEK293T cells, HEK293T cells transfected with L-plastin (WT), L-plastin Ser5Ala (S5/A), L-plastin Ser5Ala-Ser7Ala (S5-7/A) or L-plastin Ser5Glu (S/E) after 30 minutes. The arrow indicates the peak position of HEK293T cells after 0 minutes of aggregation (not shown). (D) Wound healing assay. 2D-migration of cells expressing wild-type L-plastin is similar to cells expressing mutant L-plastin. MT, mock-transfected HEK293T cells. The migration distance in μm (*y*-axis) as a function of time in hours (*x*-axis) is shown. Data are representative for two independent experiments. (E) PKA but not PKC inhibitors block L-plastin-induced invasion of HEK293T cells. Transfected cells expressing wild-type L-plastin were tested for their capacity to invade a collagen-type-I gel as described in B with the exception that PKC inhibitors (GF109 or Gö796) or PKA (KT5720) inhibitors (all at 10 μM) were present during the assay. Control, untransfected cells. –inhibitor, untreated cells expressing wild-type L-plastin. Results are representative of three independent experiments (mean ± s.d.). (F) PKA activation increases phosphorylation of L-plastin wild-type in HEK293T cells. Transfected HEK293T cells were incubated for 45 minutes in the absence (–) or in the presence (+) of PKA inhibitor H-89 and stimulated for an additional 45 minutes with 1 mM 8-Bromo-cAMP. Equal amounts of cell lysates were analysed by immunoblotting using anti-Ser5-*P* antibody (upper panel) or anti-sv-tag antibody (lower panel).

phosphorylation of L-plastin is triggered by signals activating immune cells (Henning et al., 1994; Jones and Brown, 1996; Matsushima et al., 1988; Paclet et al., 2004), pathways controlling L-plastin phosphorylation may be constitutively activated in adherent fibroblasts and epithelial cells (Lin et al., 1998). Consistently, constitutive phosphorylation was observed in activated, adherent macrophages and leucocytes (Jones and Brown, 1996; Messier et al., 1993). Phosphorylated L-plastin preferentially localised to F-actin structures, including peripheral microspikes and membrane extensions, focal adhesions and, to a lesser extent, stress fibres. This result matches previous biochemical data, revealing phosphorylated L-plastin in the detergent-resistant fraction of adherent macrophages (Messier et al., 1993). Phosphorylation on Ser residues was proposed to be required for targeting L-plastin to the actin cytoskeleton (Messier et al., 1993). We found that also non-phosphorylated L-plastin weakly colocalised with actin-rich structures. However, by marked contrast, the Ser5Glu variant highly concentrated in actin-rich plasma membrane extensions, even when expressed at low levels, whereas the Ser5Ala variant exhibited a diffuse staining, reflecting a large pool of unbound protein. This difference in staining pattern was neither due to increased degradation of L-plastin containing the Ser5Ala mutation, as monitored by immunoblotting analysis, nor to impaired F-actin binding, as suggested by our in vitro data.

Taken together, our data suggest that phosphorylation of L-plastin increases its avidity for F-actin structures in cells – as also supported by our detergent-extraction experiments. However, we cannot exclude that targeting of phosphorylated L-plastin is mediated in part by other protein partners – as demonstrated for other CH-domain family members such as ABP 280 (Goldmann, 2001). Alternatively, phosphorylation-dependent binding of L-plastin to a protein ligand may increase its actin-binding or bundling activity, consequently influencing its intracellular location. In support of such a possibility, Iba1, a Ca^{2+}-binding protein, increases the bundling activity of L-plastin in vitro (Kanazawa et al., 2002; Ohsawa et al., 2004). Although these mechanisms are not mutually exclusive, we favour a mechanism by which phosphorylation influences targeting of L-plastin by promoting its F-actin-binding property, as supported by our finding that Ser5 phosphorylation or Ser5Glu substitution increases binding to F-actin in vitro. This result also demonstrates that negatively charged residues can mimic phosphorylation, without excluding, however, that behaviours of the Ser5Glu variant and of phosphorylated wild-type L-plastin might be similar but not identical. The non-hydrolysable negatively charged glutamate residue might keep the Ser5Glu variant in a locked state on the filament, thereby creating the more pronounced phenotype we observed with this mutant in transfected cells. Conversely, switching the wild type from a phosphorylated and to a non-phosphorylated state might increase its off-rate.

In most of the other F-actin binding proteins, phosphorylation sites are located at an F-actin interface where the negatively charged phosphate group negatively interferes with actin binding (Azim et al., 1995; Harbeck et al., 2000; Izaguirre et al., 2001). By contrast, Ser5 phosphorylation of L-plastin occurs in the regulatory Ca^{2+}-binding headpiece-domain and promotes F-actin-binding and -bundling. Although this domain is not required for filament cross-linking, it yet increases the stiffness of actin bundles (Klein et al., 2004). Based on our data and structural information (Klein et al., 2004; Volkmann et al., 2001), Ser5 phosphorylation might induce a conformational change in the headpiece domain that affects the interaction of the actin-binding domains with actin. An increase in bundling activity was observed at low L-plastin to actin ratios where amounts of the bound non-phosphorylated L-plastin or the Ser5Glu variant were similar, suggesting that the Ser5Glu variant more efficiently promoted cross-link formation. Notably, the binding curve of Ser5Glu to F-actin did not fit a first-order reaction indicating the existence of different L-plastin or F- actin binding states. Our results do not favour a mechanism where phosphorylation would influence the Ca^{2+}-sensitivity of the F-actin bundling activity of L-plastin. Taken together, these results suggested that, although not an absolute requirement for L-plastin binding to F-actin, phosphorylation on Ser5 promotes binding and, thereby, targeting to actin-rich structures in cells.

Using a collagen invasion assay, we found that expression of L-plastin endows HEK293T cells with invasive properties. This is consistent with previous data showing that L-plastin repression by an RNA antisense approach decreased the invasive capacity of prostate carcinoma cells (Zheng et al., 1999). Cell invasion depended on Ser5 phosphorylation, suggesting that targeting of L-plastin to peripheral actin-rich membrane extensions and adhesions was required for this process. Cell migration in a 2D-space relies on coordinated cycles of cell extension, cell adhesion and actin-myosin contraction (Friedl, 2004). The fact that neither wild-type L-plastin nor L-plastin Ser5Glu increased the rate of cell migration in a wound healing assay, suggested that forced expression of these proteins does not grossly affect these processes. Because of the high transient-transfection rate we obtained in HEK293T cells (60–70%), it is unlikely that this result is caused by the low percentage of transfected cells present at the wound borders. In contrast to 2D cell movement, migration through a collagen matrix frequently involves matrix degradation by specific cell-surface proteases (Friedl, 2004). In macrophages, phosphorylated L-plastin localises to podosomes (Babb et al., 1997; Evans et al., 2003; Messier et al., 1993), plasma membrane protrusions involved in the regulation of adhesion, cell surface proteases (Buccione et al., 2004) and cancer cell invasion (Linder and Aepfelbacher, 2003). Phosphorylated L-plastin or the Ser5Glu variant did not colocalise with cortactin in podosome-like adhesion structures, yet both proteins co-distributed in membrane extensions and peripheral microspike adhesions where actin assembly occurs (Schirenbeck et al., 2005; Svitkina et al., 2003). Based on our in vitro F-actin-binding data and the observation that L-plastin Ser5Glu but not L-plastin Ser5Ala promoted formation of F-actin spikes, it is tempting to speculate that phosphorylated L-plastin might, by stabilising actin filaments, affect the assembly of membrane specialisations implicated in invasion. In line, the closely related T-plastin isoform promotes Arp2/3-mediated actin assembly and force generation in a biomimetic actin-based motility assay (Giganti et al., 2005). Alternatively, phosphorylated L-plastin might act as a scaffold for cytoskeleton-associated signalling complexes. In support of such a mechanism, L-plastin-deficient ($L\text{-plastin}^{-/-}$) polynuclear monocytes (Chen et al., 2003) exhibited a marked reduction in phosphorylation of paxillin, an cortactin-

interacting protein (Bowden et al., 1999) and Syk, a Src-kinase family member (Frame et al., 2002), signalling proteins involved in actin remodelling and cell invasion. These potential mechanisms might also account for the effect of L-plastin on cell cohesion, observed in the fast cell aggregation assay. Notably, filamin, a CH-domain actin-membrane linker protein, is required for the concentration and release of the protease epithin at cell-cell contacts (Kim et al., 2005).

PKA but not PKC inhibitors blocked L-plastin-induced collagen invasion. However, albeit PKA-mediated phosphorylation of L-plastin could be stimulated in HEK293T cells, we were unable to inhibit base-line phosphorylation. Several, non-exclusive explanations might account for these apparently discrepant results. Turnover of phosphate in L-plastin might be rather slow and longer incubation times with inhibitors, as in invasion assays, might be required to yield non-phosphorylated L-plastin. Alternatively, other, so far unknown kinases might phosphorylate L-plastin on Ser5 in HEK293T cells. Third, inhibition of PKA does affect invasion by targeting other phospho-proteins, as supported by previous studies (Howe, 2004). Further experiments are required to dissect signalling pathways linking L-plastin phosphorylation to invasion.

L-plastin is, so far, the only of the three plastin isoforms that is phosphorylated in cells (de Arruda et al., 1990; Lin et al., 1998). Unlike I-plastin and T-plastin, which are associated with relatively stable structures, such as the brush border microvilli or the stereocilia of the inner ear (Bretscher, 1981; Sobin and Flock, 1983), L-plastin might, during evolution, have acquired a specific regulatory system coupling the activity state of the protein to signalling cascades triggering events that require the rearrangement of the actin cytoskeleton (Henning et al., 1994; Jones and Brown, 1996; Matsushima et al., 1988; Shibata et al., 1993). Notably, plastins/fimbrins of various organisms harbour negatively charged residues in their N-terminal part that might have a function similar to phosphorylated Ser5 in L-plastin.

To conclude, phosphorylation of L-plastin increases its F-actin-binding affinity and is required for its efficient targeting to sites of actin assembly at the plasma membrane and for eliciting cell invasion. Our findings pave the way for further investigations of how phosphorylated L-plastin contributes to cell migration in a 3D-space during tumour cell invasion and embryonic development.

Materials and Methods

Cell cultures

Vero monkey kidney, epithelial HEK293T or LLCPK1 cells were grown in Dulbecco's modified Eagle's medium. Jurkat T lymphoid cells were maintained in RPMI 1640 medium (Bio Whittaker Europe, Verviers, Belgium). Media were supplemented with 10% fetal calf serum and cells were grown at 37°C in 5% CO_2.

Antibodies and reagents

Polyclonal rabbit IgGs against L-plastin have been previously characterised (Lapillonne et al., 2000). Mouse monoclonal anti-vinculin antibody was a kind gift of M. Glukhova (Institut Curie, Paris, France); anti-cortactin antibody was purchased from Upstate (TE Huissen, The Netherlands) and anti-vimentin antibody from Santa Cruz Biotechnology (Tebu-Bio, Boechout, Belgium). Polyclonal anti-Ser5-*P* antibody against L-plastin phosphorylated at Ser5 was raised against a peptide encoding L-plastin residues 2-17 in which Ser5 was phosphorylated (ARG**S(*P*)**VSDEEMMELREA). Rabbit antiserum was purified by negative affinity on non-phosphorylated peptide followed by positive affinity on the phosphorylated peptide. The monoclonal VII-E-7 antibody against the 13 C-terminal residues of the Sendai virus L protein (sv-tag) was a kind gift of J. Neubert (Max-Planck-Institut für Biochemie, Martinsried, Germany). The rabbit polyclonal antibody against the same sequence was described previously (Arpin et al., 1994). The anti-rabbit IgG antibody coupled to horseradish peroxidase was purchased from Amersham Biosciences (Roosendaal, The Netherlands). Cy2-conjugated goat anti-rabbit IgG was purchased from Jackson Immuno-Research Laboratories (De Pinte, Belgium). Alexa Fluor 350- or 594-coupled phalloidin and secondary antibodies were purchased from Molecular Probes (Invitrogen, Merelbeke, Belgium). β-G-actin was purchased from Cytoskeleton (Boechout, Belgium). PKA catalytic subunit, PKA activator 8-Bromo-cAMP, PKA inhibitors H89 and KT5720 and PKC inhibitor GF109 and Gö6796 were purchased from Calbiochem (Leuven, Belgium). Forskolin was obtained from Sigma (Bornem, Belgium). Lipofectin reagent was purchased from Invitrogen.

Site-directed mutagenesis of cDNAs

To mutate Ser5 into Ala or a Glu by a PCR-based approach, Mut5A (5′-AAA-AATGGCCAGAGGAGCAGTGTCC-3′), Mut5E (5′-AAAAATGGCCAGAGGA-GAAGTGTCC-3′) sense primers corresponding to L-plastin nucleotides 4-21 were used. Underlined sequences indicate mutated amino acids. The common reverse primer (3′-CTTCCCCTCCTTCAGGTCCTCAGC-5′) was complementary to bases 802-780 of L-plastin cDNA and flanked at its 5′-end by an *Nco*I site. The PCR fragment containing the mutation was used to replace the corresponding fragment of the L-plastin cDNA inserted in the pCB6 expression vector, downstream of the cytomegalovirus promoter. The Ser5Glu and Ser5Ala cDNAs were also cloned into the *BamH*I-*EcoR*I sites of the pGEX-2T expression vector. Mutated DNAs were verified by sequencing.

Recombinant proteins

Wild-type human L-plastin, as well as the Ser5Glu and Ser5Ala variants of L-plastin were produced in *E. coli* from the pGEX-2T expression vector and purified as described previously (Arpin et al., 1994). The concentration of thrombin-cleaved proteins was determined according to the Bradford method (BioRad, Nazareth, Belgium) and by SDS polyacrylamide gel electrophoresis (PAGE) using a BSA protein standard curve.

Transient expression of cDNAs in cells

Five or 10 μg of cDNA encoding wild-type human L-plastin or L-plastin variants was transfected respectively into HEK239T cells using calcium phosphate procedure (Chen and Okayama, 1988) or into 5×10^6 Vero cells by electroporation at 240 volt and 950 μF (Toneguzzo et al., 1986). LLCPK1 cells were transfected by Lipofectin.

Treatment of cells with pharmacological agents

Cells were washed with PBS and resuspended in $HBSS^{++}$ (1× Hanks' buffered salt solution) containing 20 mM Hepes, 0.5 mM Mg^{2+} and 1.0 mM Ca^{2+}. Jurkat T lymphoid cells or HEK293T cells were treated with PKA or PKC activators or inhibitors as indicated in the figure legends and described (Wang and Brown, 1999). After treatment, cells were lysed and processed for immunoblotting analysis.

Analysis of L-plastin or L-plastin variants by immunoblotting

Cells were lysed for 30 minutes in ice-cold RIPA buffer (50 mM Tris-HCl pH 7.4, 150 mM NaCl, 0.1% SDS, 1% Triton X-100, 1% NP40 and 1% Na-deoxycholate) containing a cocktail of protease and phosphatase inhibitors. Lysates were cleared by centrifugation in a microfuge at 16,000 ***g*** for 10 minutes at 4°C, and the protein concentration was determined using a modified Lowry method or Bradford assay (BioRad).

Total cell lysates (20 μg of protein) were separated by PAGE under reducing conditions and transferred onto nitrocellulose membrane (Schleicher & Schuell) using a semi-dry transblot apparatus. Primary antibodies indicated in figure legends were revealed by using secondary antibodies coupled to horseradish peroxidase and enhanced chemiluminescence (ECL). In some experiments, the membrane was stripped as previously described (Janji et al., 1999).

Indirect immunofluorescence

Transfected cells were fixed with 3% paraformaldehyde and processed for immunofluorecence labelling as described previously (Friederich et al., 1999). Labelled cells were analysed by epifluorescence microscopy (Leica DMRX microscope, HCX PL APO ×63 or ×100) or a Zeiss laser scanning confocal microscope (LSM-510 Meta). Images were acquired with a linear CCD camera (micromax, Princeton Instruments) and analysed with Metaview or Metamorph software (Universal Imaging Cooperation)

Detergent extraction of cells

Transfected Vero cells were plated onto glass coverslips. After 48 hours, coverslips were cut in halves. One half was directly processed for indirect immunofluorescence, while the other was detergent-extracted with 0.5% Triton X-100 for 16 seconds at 20°C, as previously described (Arpin et al., 1994; Friederich et al., 1992) and then processed for immunofluorescence labelling. For quantification, number of cells with detectable sv-tag labelling per 100 cells were determined for each half coverslip,

yielding quantitative information on the transfection efficiency and on the resistance of transfected proteins to detergent extraction.

Phosphorylation of L-plastin in vitro

L-plastin protein was phosphorylated using PKA catalytic subunit (specific activity ⩾750 units/μg of protein) at 30°C in a reaction mixture containing 20 mM Tris-HCl pH 7.4, 20 mM $MgCl_2$, 10 mM dithiothreitol and 100 μM ATP. To monitor phosphorylation, aliquots were removed, the reaction was stopped by addition of boiling SDS-sample buffer and proteins were analysed by immunoblotting following the ECL detection method (Amersham Bioscience). To analyse F-actin binding capacity of L-plastin, aliquots from the reaction were added to G-actin and processed as described below.

Actin binding and bundling assays

G-actin was polymerised overnight at 4°C or for 4 hours at room temperature in the presence of L-plastin variants in polymerisation buffer (100 mM KCl, 1 mM $MgCl_2$, 1 mM ATP, 0.5 mM EGTA, 50 mM sodium phosphate buffer, pH 7.0) as indicated in figure legends. Sedimentation of actin filaments and L-plastin was achieved by high-speed centrifugation at 200,000 ***g*** for 30 minutes. To sediment actin bundles, samples were centrifuged for 15 minutes at 12,000 ***g*** (Glenney, Jr et al., 1981). Proteins in pellets and supernatants were separated by SDS-PAGE. Coomassie-stained protein bands were scanned and densities were quantified using BioCapt and Bio-PROFIL Bio 1D software (Windows applications) or LabImage software 2.7.2 (Kapelan Bio-Imaging Solution).

Transmission electron microscopy

Samples prepared for the above-described bundling assay were analysed by transmission electron microscopy. Aliquots were removed from the mixture before centrifugation and immediately negatively stained with 1% uranyl acetate. Electron micrographs were obtained using a Philips CM 120 microscope at a magnification of 28,000× or 45,000×.

Collagen invasion assays

Gels were prepared in a six-well plate from a collagen-type -I solution (Upstate Biotechnology, Lake Placid, NY). Cells (1×10^5) were incubated on top of the gels for 24 hours at 37°C. HEK293T cells inside the gel were scored with a phase contrast microscope controlled by a computer program (Bracke et al., 2001; De Corte et al., 2002). Invasive and superficial cells were counted in 12 fields of 0.157 mm^2. The invasion index is the percentage of cells invading the gel over the total number of cells counted. DHD-FIB rat colon myofibroblasts were used as a positive control. Experiments were performed in triplicate. Mean values and standard deviations were calculated.

Fast aggregation assay

Cell-cell adhesion was numerically evaluated in an aggregation assay as described earlier (Boterberg et al., 2001). Briefly, single-cell suspensions of HEK293T cells were prepared according to an N-cadherin-saving procedure and allowed to aggregate on a Gyrotory shaker at 80 rpm for 30 minutes in aggregation buffer (1.25 mM Ca^{2+}, 0.1 mg DNase /ml, 10 mM Hepes and 0.1% BSA) and equilibrated at physiological pH and osmolarity. Cell aggregation was measured with an LS particle size analyzer (LS 200, Coulter Electronics) after 0 and 30 minutes of aggregation. The relative volume in function of the particle size was used as an index of aggregation. Semi-quantitative evaluation of Fast Aggregation (FA) was determined as follow. Less than 20 μm, no aggregates I; between 20 and 100 μm, no aggregates II; between 100 and 1000 μm, aggregates III; more than 1000 μm, aggregates IV.

Wound healing assay

HEK293T cells (8×10^5) were seeded into six-well cell culture plates and 18 hours after seeding, cells were transfected with cDNA constructs. After 48 hours, a wound was made by scratching a line in a confluent monolayer. Cell debris was removed by washing the cells with serum-free medium. Migration of cells into the wound was then observed at different time points. Cells were followed for 24 hours.

We wish to thank M. Goethals and L. Cabanié for their excellent technical help. This work was supported by the Centre National de Recherche Scientifique, France, the 'Fondation Luxembourgeoise Contre le Cancer', the Fondation 'Aide aux enfants atteints d'un cancer, Luxembourg'. A.G. is supported by fellowships from the MCESR, Lions Vaincre le Cancer, Luxembourg and by a grant of the EMBO Advanced Light Microscopy Facility. J.G. and V.D.C. greatly appreciate support from Marc Mareel and Joël Vandekerckhove, and acknowledge support of the Interuniversity Attraction Poles (IUAP/P5), Fortis Bank Verzekeringen, and the Belgian Federation against Cancer. V.D.C. is a Postdoctoral Fellow of the Fund for Scientific Research-Flanders, Belgium (F.W.O.).

References

Arpin, M., Friederich, E., Algrain, M., Vernel, F. and Louvard, D. (1994). Functional differences between L- and T-plastin isoforms. *J. Cell Biol.* **127**, 1995-2008.

Azim, A. C., Knoll, J. H., Beggs, A. H. and Chishti, A. H. (1995). Isoform cloning, actin binding, and chromosomal localization of human erythroid dematin, a member of the villin superfamily. *J. Biol. Chem.* **270**, 17407-17413.

Babb, S. G., Matsudaira, P., Sato, M., Correia, I. and Lim, S. S. (1997). Fimbrin in podosomes of monocyte-derived osteoclasts. *Cell Motil. Cytoskeleton* **37**, 308-325.

Bartles, J. R. (2000). Parallel actin bundles and their multiple actin-bundling proteins. *Curr. Opin. Cell Biol.* **12**, 72-78.

Boterberg, T., Bracke, M. E., Bruyneel, E. A. and Mareel, M. M. (2001). Cell aggregation assays. In *Methods in Molecular Medicine, Vol. 58, Metastasis Research Protocols, Vol. 2: Analysis of Cell Behaviour In Vitro and In Vivo* (ed. S. A. Brooks and U. Schumacher), pp. 33-45. Totowa, NJ: Humana Press.

Bowden, E. T., Barth, M., Thomas, D., Glazer, R. I. and Mueller, S. C. (1999). An invasion-related complex of cortactin, paxillin and PKCmu associates with invadopodia at sites of extracellular matrix degradation. *Oncogene* **18**, 4440-4449.

Bracke, M. E., Boterberg, T., Bruyneel, E. A. and Mareel, M. M. (2001). Collagen invasion assay. In *Methods in Molecular Medicine, Vol. 58, Metastasis Research Protocols, Vol. 2: Analysis of Cell Behaviour In Vitro and In Vivo* (ed. S. A. Brooks and U. Schumacher), pp. 81-89. Totowa, NJ: Humana Press.

Bretscher, A. (1981). Fimbrin is a cytoskeletal protein that crosslinks F-actin in vitro. *Proc. Natl. Acad. Sci. USA* **78**, 6849-6853.

Bryce, N. S., Clark, E. S., Leysath, J. L., Currie, J. D., Webb, D. J. and Weaver, A. M. (2005). Cortactin promotes cell motility by enhancing lamellipodial persistence. *Curr. Biol.* **15**, 1276-1285.

Buccione, R., Orth, J. D. and McNiven, M. A. (2004). Foot and mouth: podosomes, invadopodia and circular dorsal ruffles. *Nat. Rev. Mol. Cell. Biol.* **5**, 647-657.

Chen, C. A. and Okayama, H. (1988). Calcium phosphate-mediated gene transfer: a highly efficient transfection system for stably transforming cells with plasmid DNA. *Biotechniques* **6**, 632-638.

Chen, H., Mocsai, A., Zhang, H., Ding, R. X., Morisaki, J. H., White, M., Rothfork, J. M., Heiser, P., Colucci-Guyon, E., Lowell, C. A. et al. (2003). Role for plastin in host defense distinguishes integrin signaling from cell adhesion and spreading. *Immunity* **19**, 95-104.

Clarke, D. M., Brown, M. C., LaLonde, D. P. and Turner, C. E. (2004). Phosphorylation of actopaxin regulates cell spreading and migration. *J. Cell Biol.* **166**, 901-912.

Correia, I., Chu, D., Chou, Y. H., Goldman, R. D. and Matsudaira, P. (1999). Integrating the actin and vimentin cytoskeletons. adhesion-dependent formation of fimbrin-vimentin complexes in macrophages. *J. Cell Biol.* **146**, 831-842.

de Arruda, M. V., Watson, S., Lin, C. S., Leavitt, J. and Matsudaira, P. (1990). Fimbrin is a homologue of the cytoplasmic phosphoprotein plastin and has domains homologous with calmodulin and actin gelation proteins. *J. Cell Biol.* **111**, 1069-1079.

De Corte, V., Bruyneel, E., Boucherie, C., Mareel, M., Vandekerckhove, J. and Gettemans, J. (2002). Gelsolin-induced epithelial cell invasion is dependent on Ras-Rac signaling. *EMBO J.* **21**, 6781-6790.

Evans, J. G., Correia, I., Krasavina, O., Watson, N. and Matsudaira, P. (2003). Macrophage podosomes assemble at the leading lamella by growth and fragmentation. *J. Cell Biol.* **161**, 697-705.

Frame, M. C., Fincham, V. J., Carragher, N. O. and Wyke, J. A. (2002). v-Src's hold over actin and cell adhesions. *Nat. Rev. Mol. Cell Biol.* **3**, 233-245.

Friederich, E., Huet, C., Arpin, M. and Louvard, D. (1989). Villin induces microvilli growth and actin redistribution in transfected fibroblasts. *Cell* **59**, 461-475.

Friederich, E., Vancompernolle, K., Huet, C., Goethals, M., Finidori, J., Vandekerckhove, J. and Louvard, D. (1992). An actin-binding site containing a conserved motif of charged amino acid residues is essential for the morphogenic effect of villin. *Cell* **70**, 81-92.

Friederich, E., Vancompernolle, K., Louvard, D. and Vandekerckhove, J. (1999). Villin function in the organization of the actin cytoskeleton. Correlation of in vivo effects to its biochemical activities in vitro. *J. Biol. Chem.* **274**, 26751-26760.

Friedl, P. (2004). Prespecification and plasticity: shifting mechanisms of cell migration. *Curr. Opin. Cell Biol.* **16**, 14-23.

Gautreau, A., Louvard, D. and Arpin, M. (2000). Morphogenic effects of ezrin require a phosphorylation-induced transition from oligomers to monomers at the plasma membrane. *J. Cell Biol.* **150**, 193-203.

Giganti, A. and Friederich, E. (2003). The actin cytoskeleton as a therapeutic target: state of the art and future directions. *Prog. Cell Cycle Res.* **5**, 511-525.

Giganti, A., Plastino, J., Janji, B., Van Troys, M., Lentz, D., Ampe, C., Sykes, C. and Friederich, E. (2005). Actin-filament cross-linking protein T-plastin increases Arp2/3-mediated actin-based movement. *J. Cell Sci.* **118**, 1255-1265.

Gimona, M., Djinovic-Carugo, K., Kranewitter, W. J. and Winder, S. J. (2002). Functional plasticity of CH domains. *FEBS Lett.* **513**, 98-106.

Glenney, J. R., Jr, Kaulfus, P., Matsudaira, P. and Weber, K. (1981). F-actin binding and bundling properties of fimbrin, a major cytoskeletal protein of microvillus core filaments. *J. Biol. Chem.* **256**, 9283-9288.

Goldmann, W. H. (2001). Phosphorylation of filamin (ABP-280) regulates the binding to the lipid membrane, integrin, and actin. *Cell Biol. Int.* **25**, 805-808.

Goldstein, D., Djeu, J., Latter, G., Burbeck, S. and Leavitt, J. (1985). Abundant synthesis of the transformation-induced protein of neoplastic human fibroblasts, plastin, in normal lymphocytes. *Cancer Res.* **45**, 5643-5647.

Harbeck, B., Huttelmaier, S., Schluter, K., Jockusch, B. M. and Illenberger, S. (2000).

Phosphorylation of the vasodilator-stimulated phosphoprotein regulates its interaction with actin. *J. Biol. Chem.* **275**, 30817-30825.

Henning, S. W., Meuer, S. C. and Samstag, Y. (1994). Serine phosphorylation of a 67-kDa protein in human T lymphocytes represents an accessory receptor-mediated signaling event. *J. Immunol.* **152**, 4808-4815.

Howe, A. K. (2004). Regulation of actin-based cell migration by cAMP/PKA. *Biochim. Biophys. Acta* **1692**, 159-174.

Huttelmaier, S., Harbeck, B., Steffens, O., Messerschmidt, T., Illenberger, S. and Jockusch, B. M. (1999). Characterization of the actin binding properties of the vasodilator-stimulated phosphoprotein VASP. *FEBS Lett.* **451**, 68-74.

Izaguirre, G., Aguirre, L., Hu, Y. P., Lee, H. Y., Schlaepfer, D. D., Aneskievich, B. J. and Haimovich, B. (2001). The cytoskeletal/non-muscle isoform of alpha-actinin is phosphorylated on its actin-binding domain by the focal adhesion kinase. *J. Biol. Chem.* **276**, 28676-28685.

Janji, B., Melchior, C., Gouon, V., Vallar, L. and Kieffer, N. (1999). Autocrine TGF-beta-regulated expression of adhesion receptors and integrin-linked kinase in HT-144 melanoma cells correlates with their metastatic phenotype. *Int. J. Cancer* **83**, 255-262.

Jones, S. L. and Brown, E. J. (1996). FcgammaRII-mediated adhesion and phagocytosis induce L-plastin phosphorylation in human neutrophils. *J. Biol. Chem.* **271**, 14623-14630.

Jones, S. L., Wang, J., Turck, C. W. and Brown, E. J. (1998). A role for the actin-bundling protein L-plastin in the regulation of leukocyte integrin function. *Proc. Natl. Acad. Sci. USA* **95**, 9331-9336.

Kanazawa, H., Ohsawa, K., Sasaki, Y., Kohsaka, S. and Imai, Y. (2002). Macrophage/microglia-specific protein Iba1 enhances membrane ruffling and Rac activation via phospholipase C-gamma-dependent pathway. *J. Biol. Chem.* **277**, 20026-20032.

Kim, C., Cho, Y., Kang, C. H., Kim, M. G., Lee, H., Cho, E. G. and Park, D. (2005). Filamin is essential for shedding of the transmembrane serine protease, epithin. *EMBO Rep.* **6**, 1045-1051.

Klein, M. G., Shi, W., Ramagopal, U., Tseng, Y., Wirtz, D., Kovar, D. R., Staiger, C. J. and Almo, S. C. (2004). Structure of the actin crosslinking core of fimbrin. *Structure* **12**, 999-1013.

Lapillonne, A., Coue, O., Friederich, E., Nicolas, A., Del Maestro, L., Louvard, D., Robine, S. and Sastre-Garau, X. (2000). Expression patterns of L-plastin isoform in normal and carcinomatous breast tissues. *Anticancer Res.* **20**, 3177-3182.

Lin, C. S., Chen, Z. P., Park, T., Ghosh, K. and Leavitt, J. (1993a). Characterization of the human L-plastin gene promoter in normal and neoplastic cells. *J. Biol. Chem.* **268**, 2793-2801.

Lin, C. S., Park, T., Chen, Z. P. and Leavitt, J. (1993b). Human plastin genes. Comparative gene structure, chromosome location, and differential expression in normal and neoplastic cells. *J. Biol. Chem.* **268**, 2781-2792.

Lin, C. S., Lau, A. and Lue, T. F. (1998). Analysis and mapping of plastin phosphorylation. *DNA Cell Biol.* **17**, 1041-1046.

Linder, S. and Aepfelbacher, M. (2003). Podosomes: adhesion hot-spots of invasive cells. *Trends Cell. Biol.* **13**, 376-385.

Loomis, P. A., Zheng, L., Sekerkova, G., Changyaleket, B., Mugnaini, E. and Bartles, J. R. (2003). Espin cross-links cause the elongation of microvillus-type parallel actin bundles in vivo. *J. Cell Biol.* **163**, 1045-1055.

Matsushima, K., Shiroo, M., Kung, H. F. and Copeland, T. D. (1988). Purification and characterization of a cytosolic 65-kilodalton phosphoprotein in human leukocytes whose phosphorylation is augmented by stimulation with interleukin 1. *Biochemistry* **27**, 3765-3770.

Messier, J. M., Shaw, L. M., Chafel, M., Matsudaira, P. and Mercurio, A. M. (1993). Fimbrin localized to an insoluble cytoskeletal fraction is constitutively phosphorylated on its headpiece domain in adherent macrophages. *Cell Motil. Cytoskeleton* **25**, 223-233.

Mizutani, K., Miki, H., He, H., Maruta, H. and Takenawa, T. (2002). Essential role of neural Wiskott-Aldrich syndrome protein in podosome formation and degradation of extracellular matrix in src-transformed fibroblasts. *Cancer Res.* **62**, 669-674.

Namba, Y., Ito, M., Zu, Y., Shigesada, K. and Maruyama, K. (1992). Human T cell L-plastin bundles actin filaments in a calcium-dependent manner. *J. Biochem.* **112**, 503-507.

Ohsawa, K., Imai, Y., Sasaki, Y. and Kohsaka, S. (2004). Microglia/macrophage-specific protein Iba1 binds to fimbrin and enhances its actin-bundling activity. *J. Neurochem.* **88**, 844-856.

Paclet, M. H., Davis, C., Kotsonis, P., Godovac-Zimmermann, J., Segal, A. W. and Dekker, L. V. (2004). N-Formyl peptide receptor subtypes in human neutrophils activate L-plastin phosphorylation through different signal transduction intermediates. *Biochem. J.* **377**, 469-477.

Park, T., Chen, Z. P. and Leavitt, J. (1994). Activation of the leukocyte plastin gene occurs in most human cancer cells. *Cancer Res.* **54**, 1775-1781.

Pollard, T. D. and Borisy, G. G. (2003). Cellular motility driven by assembly and disassembly of actin filaments. *Cell* **112**, 453-465.

Rosales, C., Jones, S. L., McCourt, D. and Brown, E. J. (1994). Bromophenacyl bromide binding to the actin-bundling protein l-plastin inhibits inositol trisphosphate-independent increase in Ca^{2+} in human neutrophils. *Proc. Natl. Acad. Sci. USA* **91**, 3534-3538.

Samstag, Y., Eibert, S. M., Klemke, M. and Wabnitz, G. H. (2003). Actin cytoskeletal dynamics in T lymphocyte activation and migration. *J. Leukoc. Biol.* **73**, 30-48.

Schirenbeck, A., Bretschneider, T., Arasada, R., Schleicher, M. and Faix, J. (2005). The Diaphanous-related formin dDia2 is required for the formation and maintenance of filopodia. *Nat. Cell Biol.* **7**, 619-625.

Shibata, M., Ohoka, T., Mizuno, S. and Suzuki, K. (1993). Characterization of a 64-kd protein phosphorylated during chemotactic activation with IL-8 and fMLP of human polymorphonuclear leukocytes. I. Phosphorylation of a 64-kd protein and other proteins. *J. Leukoc. Biol.* **54**, 1-9.

Shinomiya, H., Hagi, A., Fukuzumi, M., Mizobuchi, M., Hirata, H. and Utsumi, S. (1995). Complete primary structure and phosphorylation site of the 65-kDa macrophage protein phosphorylated by stimulation with bacterial lipopolysaccharide. *J. Immunol.* **154**, 3471-3478.

Sobin, A. and Flock, A. (1983). Immunohistochemical identification and localization of actin and fimbrin in vestibular hair cells in the normal guinea pig and in a strain of the waltzing guinea pig. *Acta Otolaryngol.* **96**, 407-412.

Stossel, T. P., Condeelis, J., Cooley, L., Hartwig, J. H., Noegel, A., Schleicher, M. and Shapiro, S. S. (2001). Filamins as integrators of cell mechanics and signalling. *Nat. Rev. Mol. Cell Biol.* **2**, 138-145.

Svitkina, T. M., Bulanova, E. A., Chaga, O. Y., Vignjevic, D. M., Kojima, S., Vasiliev, J. M. and Borisy, G. G. (2003). Mechanism of filopodia initiation by reorganization of a dendritic network. *J. Cell Biol.* **160**, 409-421.

Toneguzzo, F., Hayday, A. C. and Keating, A. (1986). Electric field-mediated DNA transfer: transient and stable gene expression in human and mouse lymphoid cells. *Mol. Cell. Biol.* **6**, 703-706.

Volkmann, N., DeRosier, D., Matsudaira, P. and Hanein, D. (2001). An atomic model of actin filaments cross-linked by fimbrin and its implications for bundle assembly and function. *J. Cell Biol.* **153**, 947-956.

Wang, J. and Brown, E. J. (1999). Immune complex-induced integrin activation and L-plastin phosphorylation require protein kinase A. *J. Biol. Chem.* **274**, 24349-24356.

Weed, S. A., Karginov, A. V., Schafer, D. A., Weaver, A. M., Kinley, A. W., Cooper, J. A. and Parsons, J. T. (2000). Cortactin localization to sites of actin assembly in lamellipodia requires interactions with F-actin and the Arp2/3 complex. *J. Cell Biol.* **151**, 29-40.

Zheng, J., Rudra-Ganguly, N., Powell, W. C. and Roy-Burman, P. (1999). Suppression of prostate carcinoma cell invasion by expression of antisense L-plastin gene. *Am. J. Pathol.* **155**, 115-122.